

## An integrated monitoring system for life-cycle management of wind turbines

Kay Smarsly<sup>\*1</sup>, Dietrich Hartmann<sup>2</sup> and Kincho H. Law<sup>1</sup>

<sup>1</sup>Department of Civil and Environmental Engineering, Stanford University, Stanford, CA 94305, USA

<sup>2</sup>Department of Civil and Environmental Engineering, Ruhr-University Bochum, 44801 Bochum, Germany

(Received August 16, 2012, Revised February 2, 2013, Accepted February 10, 2013)

**Abstract.** With an annual growth rate of about 30%, wind energy systems, such as wind turbines, represent one of the fastest growing renewable energy technologies. Continuous structural health monitoring of wind turbines can help improving structural reliability and facilitating optimal decisions with respect to maintenance and operation at minimum associated life-cycle costs. This paper presents an integrated monitoring system that is designed to support structural assessment and life-cycle management of wind turbines. The monitoring system systematically integrates a wide variety of hardware and software modules, including sensors and computer systems for automated data acquisition, data analysis and data archival, a multiagent-based system for self-diagnosis of sensor malfunctions, a model updating and damage detection framework for structural assessment, and a management module for monitoring the structural condition and the operational efficiency of the wind turbine. The monitoring system has been installed on a 500 kW wind turbine located in Germany. Since its initial deployment in 2009, the system automatically collects and processes structural, environmental, and operational wind turbine data. The results demonstrate the potential of the proposed approach not only to ensure continuous safety of the structures, but also to enable cost-efficient maintenance and operation of wind turbines.

**Keywords:** life-cycle management; structural health monitoring; wind turbines; multi-agent technology; remote monitoring; damage detection; model updating; system identification

### 1. Introduction

The worldwide energy demand is rapidly increasing. According to the U.S. Energy Information Administration, the world energy consumption will increase by 53% between 2008 and 2035 (EIA 2011). The most rapid growth in energy demand will occur in non-OECD nations where, driven by strong long-term economic growth, the energy use will increase by 85% between 2008 and 2035. Given the depletion of non-renewable, natural resources such as coal, oil, and natural gas, it becomes apparent that “green” energy systems, harnessing renewable resources, are critical to meet the enormous worldwide energy demand. Financial investments in renewable energy systems have significantly increased in recent years (Feinberg 2011). For example, in 2010 the worldwide investments in renewable energy technologies, compared with 2009, have increased by 30% to \$243 billion. The major portion was spent by China with \$54 billion, followed by Germany with

---

<sup>\*</sup>Corresponding author, Postdoctoral Research Fellow, E-mail: [kay@smarsly.de](mailto:kay@smarsly.de)

\$41 billion, and the United States with \$34 billion (Schneider *et al.* 2011). According to the World Wind Energy Association, wind energy systems are currently used for power generation in 83 countries, 52 of which having increased their totally installed wind energy generation capacity in 2010 (WWEA 2012). All in all, the worldwide capacity has reached 237 GW in 2011 and is estimated to exceed 500 GW in 2015, and 1,000 GW in 2020.

Key considerations when installing wind turbines are their availability, reliability, and profitability. Generally speaking, larger wind turbines may potentially have higher failure rates and incur more downtime compared to smaller turbines. Since state-of-the-art wind turbines are continuously growing in size, the downtime caused by failures may – depending on the failure type – engender significant productivity and economic loss (Ribrant and Bertling 2007, Echavarria *et al.* 2008). Therefore, extensive research has been conducted in recent years to enhance the reliability of wind turbines for the purpose of reducing operation, repair, and maintenance costs (Lu *et al.* 2009, Amirat *et al.* 2007). Structural health monitoring (SHM) systems have been installed on wind turbines to facilitate damage detection and safety assessment of the wind turbines and wind turbine components (Swartz *et al.* 2010). By deploying SHM systems for long-term monitoring of wind turbines, maintenance and repair work can be scheduled promptly and economically, and the downtime of wind turbines can be drastically reduced.

Wind turbine monitoring represents a fertile cross-disciplinary research area comprising several research directions that involve various sophisticated technologies (Ciang *et al.* 2008, Hyers *et al.* 2006). For example, Rolfes *et al.* (2006) have used numerical modeling for damage detection; the researchers have instrumented wireless SHM systems on several wind turbines for collecting structural data to be used as the basis for damage detection (Rolfes *et al.* 2007). Many research projects focus on monitoring of specific components (or structural parts) of a wind turbine, such as rotor blades or wind turbine tower (Hameed *et al.* 2009). Considering the wind turbine tower, Avendano-Valencia *et al.* (2011) have introduced non-stationary parametric time-dependent autoregressive models for in-operation system identification of wind turbine structures. Hartmann and Höffer (2010) are investigating lifetime prediction strategies for wind turbine structures; specifically, a wind turbine tower has been instrumented with an array of sensors for long-term monitoring. The sensor system is connected to an Internet-enabled, decentralized monitoring framework that continuously processes the data sets collected from the structural system, which are then used for lifetime prediction of the wind turbine (Hartmann *et al.* 2011).

Among the requirements for accurate structural assessment and economic life-cycle management of a wind turbine is the reliable acquisition of long-term monitoring data. The data sets, which include structural responses, environmental quantities as well as operational parameters, serve as the basis not only to detect structural or operational anomalies, but also to create and update numerical and life-cycle models of the wind turbine. Therefore, the availability of a SHM system and the permanent acquisition of monitoring data with minimum interruptions are important. It is well known that malfunctions of a SHM system or breakdowns of data acquisition units and sensors can lead to undesired interruptions of the data acquisition affecting the monitoring quality considerably (Besnard 2009, Hameed *et al.* 2009, Nilsson and Bertling 2007). However, most current real-time SHM systems are not designed for fault-tolerant behavior and can suffer from component failures and system malfunctions.

This paper presents an integrated monitoring system for life-cycle management of wind turbines, which is capable of self-detecting system malfunctions and enables a reliable acquisition of sensor data needed for assessing the structural condition and operational efficiency of the wind

turbine. The integrated monitoring system, as shown in Fig. 1, consists of five basic subsystems installed at spatially distributed locations.

- i. An *on-site hardware system*, composed of sensor components, data acquisition units and a local computer (on-site server), is installed on the wind turbine to continuously collect structural, environmental, and operational data.
- ii. A *decentralized software system*, which is remotely connected to the on-site hardware system, persistently stores the data acquired by the on-site hardware system and provides remote access to the data sets.
- iii. A multiagent-based *self-diagnostic system*, capable of self-detecting system malfunctions and sensor breakdowns, ensures a reliable operation of the integrated monitoring system.
- iv. A *model updating framework* provides computational models of the wind turbine structure, which are continuously updated by means of system identification based on the sensor data from the decentralized software system.
- v. A *management module* is devised to support the wind turbine life-cycle management through remote analyses of structural, environmental, and operational wind turbine data.

Each of the modular subsystems listed above is described in details in the following sections. Examples are shown using the long-term monitoring data taken from a wind turbine, on which the integrated monitoring system has been installed in 2009. The paper concludes with a brief summary and an outlook on future research.

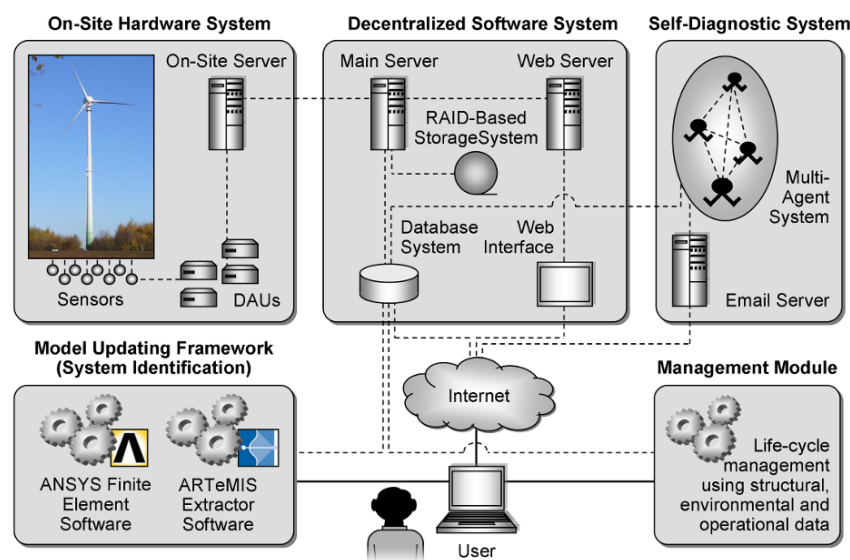


Fig. 1 Architecture of the integrated monitoring system

## 2. On-site hardware system

The on-site hardware system is installed on a 500 kW wind turbine in Germany (Fig. 2). The wind turbine tower, a zinc-coated steel shaft bolted to a concrete foundation, has a hub height of

65 m. The on-site hardware system is installed inside and outside the tower and comprises of a network of sensors, data acquisition units, and an on-site server. As shown in Fig. 3, six three-dimensional accelerometers (labeled  $B_1$  to  $B_6$ ), type PCB-3713D1FD3G, are mounted on five different levels on the inner surface of the wind turbine tower. The sensitivity of the accelerometers is 700 mV/g with a measurement range of  $\pm 3.0$  g and a frequency range between 0 and 100 Hz. Three additional accelerometers (labeled  $B_7$  to  $B_9$ ) are placed at the foundation of the wind turbine. Since very small accelerations are expected at the foundation, single-axis piezoelectric seismic ICP accelerometers, type PCB-393B12, with a sensitivity of 10,000 mV/g are used; their measurement range is  $\pm 0.5$  g.

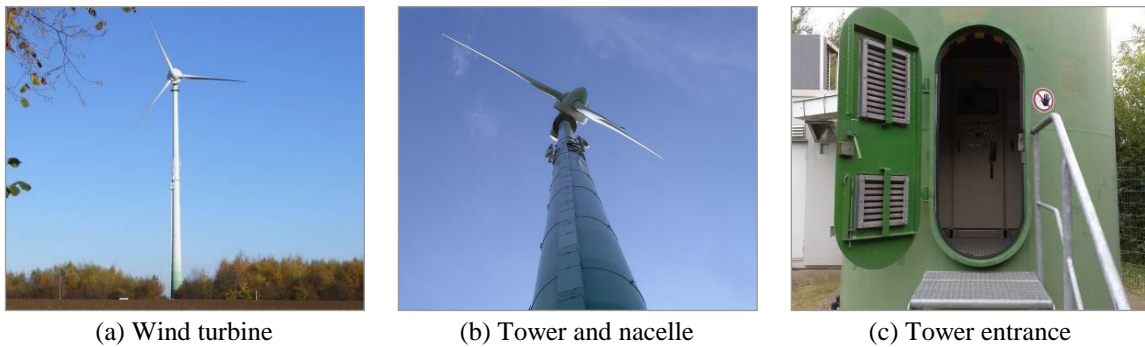


Fig. 2 Monitored wind turbine

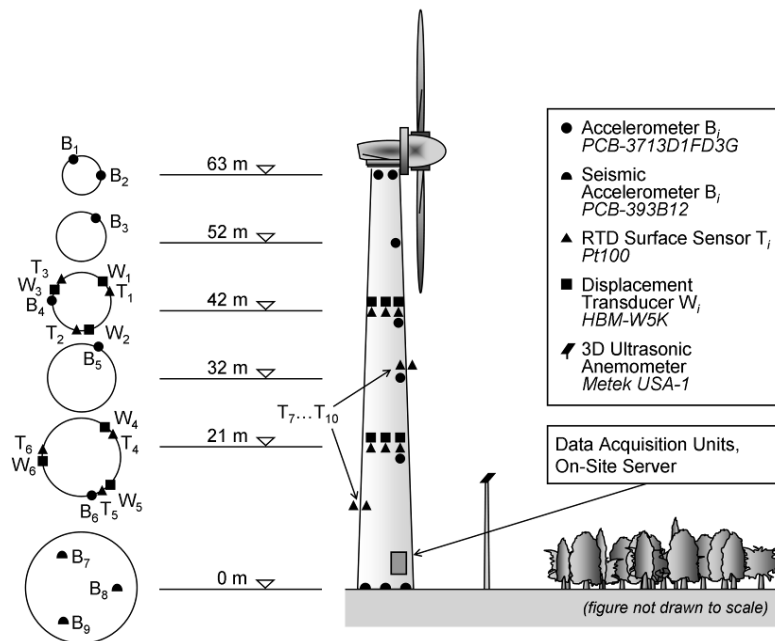
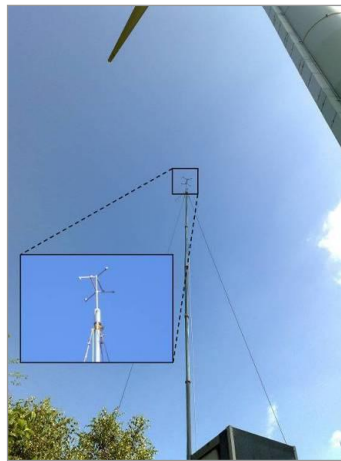


Fig. 3 Overview of the on-site hardware system

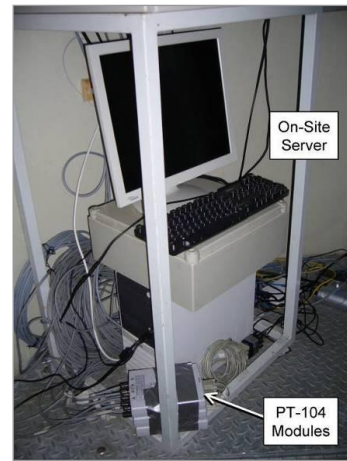
Six inductive displacement transducers HBM-W5K (labeled  $W_1$  to  $W_6$ ) with a range of 5 mm are mounted at the levels of 21 m and 42 m inside the tower. To account for temperature influences on the displacement measurements, the inductive displacement transducers are complemented by RTD surface sensors Pt100 (labeled  $T_1$  to  $T_6$ ) capable of measuring temperature from  $-60^\circ\text{C}$  to  $+200^\circ\text{C}$ . Additional temperature sensors (labeled  $T_7$  to  $T_{10}$ ) are placed inside and outside the tower to measure temperature gradients. For recording 3-dimensional wind data, a Metek USA-1 ultrasonic anemometer is mounted on a telescopic mast adjacent to the wind turbine (Fig. 4(a)).

Measuring at sampling rates up to 50 Hz, the ultrasonic anemometer records horizontal wind directions ( $0 \dots 360^\circ$ ) as well as horizontal and vertical wind speeds (from 0 to 60 m/s).

Furthermore, the anemometer collects air temperature measurements (with a range from  $-40^\circ\text{C}$  to  $+60^\circ\text{C}$ ).



(a) Ultrasonic anemometer



(b) On-site server and DAUs

Fig. 4 Devices of the on-site hardware system

To automatically collect and process the structural and environmental data, two types of data acquisition units (DAUs) are installed in the wind turbine. Each DAU is connected to the on-site server, which is also placed inside the wind turbine (Fig. 4(b)). For the acquisition of temperature data, three 4-channel Picotech RTD input modules PT-104 are deployed. The input modules are connected to the on-site server via RS232 to USB interface converters. For the acquisition of acceleration and displacement data, four Spider8 measuring units are used. Each Spider8 unit has separate A/D converters ensuring simultaneous measurements at sampling rates between 1 Hz and 9,600 Hz. All data sets, being sampled and digitized, are continuously forwarded from the DAUs to the on-site server for temporary storage. In addition to the structural and environmental sensor data collected by the DAUs, operational wind turbine data, such as power production and rotational speed, is taken directly from the wind turbine's internal supervisory control system. In addition, a nacelle-mounted cup anemometer provides continuous wind speed measurements at 67 m height. Further details on the wind turbine instrumentation can be found in Lachmann *et al.* (2009).

### 3. Decentralized software system

The decentralized software system is installed on different computers at the Institute for Computational Engineering (ICE) in Bochum, Germany. The software system is designed to serve two basic purposes: First, it provides a persistent storage for the data sets taken from the wind turbine supporting automated *data management and processing*; second, it includes a set of program modules enabling *remote access to the integrated monitoring system*.

As described previously, monitoring data collected from the wind turbine is stored temporarily on the on-site server, which creates local backups of all recorded data sets in periodic intervals. The collected raw data, referred to as “primary monitoring data”, is transmitted from the on-site server through a permanently installed DSL connection to a main server at ICE. The data transmission is automatically executed by a “Cron” job scheduler, which is a time-based Unix utility running on the on-site server to ensure the periodic execution of tasks according to scheduled time intervals. On the main server at ICE, the primary monitoring data is converted into “secondary monitoring data” that is easily interpretable by human users. The secondary monitoring data is backed up in a RAID-based storage system and then persistently stored in a MySQL database system installed at ICE. Once the data is successfully converted and stored in the database, an acknowledgement is sent from the main server at ICE to the on-site server in the wind turbine, whereupon the respective primary monitoring data on the on-site server is deleted. During the conversion process, all data sets involved are automatically “locked” and cannot be accessed by software programs or by human users in order to avoid inconsistencies. The data conversion is done at the main server using the open-source tool “Pentaho Data Integration” (Roldan 2009, Castors 2008). Performance tests validating the automated data conversion process are documented in Smarsly and Hartmann (2009a, b, 2010) and Smarsly *et al.* (2012).

Table	Records	Type	Size
pt104_3	17,806,670	MyISAM	4.4 GiB
pt104_60	946,176	MyISAM	237.7 MiB
pt104_360	148,397	MyISAM	37.3 MiB
pt104_600	94,617	MyISAM	23.8 MiB
pt104_1800	29,686	MyISAM	7.5 MiB
pt104_21600	2,477	MyISAM	638.3 KiB
spider8_3	17,475,701	MyISAM	12.9 GiB
spider8_60	944,449	MyISAM	712.8 MiB
spider8_360	145,640	MyISAM	109.9 MiB
spider8_600	94,446	MyISAM	71.3 MiB
spider8_1800	29,135	MyISAM	22.0 MiB
spider8_21600	2,434	MyISAM	1.8 MiB
usa_3	17,740,632	MyISAM	2.0 GiB
usa_60	946,001	MyISAM	107.7 MiB
usa_360	147,847	MyISAM	16.8 MiB
usa_600	94,600	MyISAM	10.8 MiB
usa_1800	29,575	MyISAM	3.4 MiB
usa_21600	2,467	MyISAM	289.0 KiB

Field	Type	Null	Default	Comments
time	bigint(20)	No		
v_least_non_outlier	float	No		
v_lower_quartile	float	No		
v_median	float	No		
v_mean	float	No		
v_upper_quartile	float	No		
v_largest_non_outlier	float	No		
d_least_non_outlier	float	No		
d_lower_quartile	float	No		
d_median	float	No		
d_mean	float	No		
d_upper_quartile	float	No		
d_largest_non_outlier	float	No		
z_least_non_outlier	float	No		
z_lower_quartile	float	No		
z_median	float	No		
z_mean	float	No		
z_upper_quartile	float	No		
z_largest_non_outlier	float	No		
t_least_non_outlier	float	No		
t_lower_quartile	float	No		
t_median	float	No		
t_mean	float	No		
t_upper_quartile	float	No		
t_largest_non_outlier	float	No		

Fig. 5 Tertiary monitoring data composed of characteristic values (database structure)

Once being stored in the MySQL database system at ICE, the secondary monitoring data is available to remotely connected and authorized human users as well as software programs for further data analyses. With respect to the database structure, two database tables “pt104” and “spider8” are defined, which correspond to the two types of DAUs, the PT-104 modules and Spider8 measuring units, installed in the wind turbine. A third database table, named “usa”, is used to manage the secondary monitoring data originating from the USA-1 ultrasonic anemometer. Each field in a database table represents one sensor connected to the DAU. During the automated conversion process, “tertiary monitoring data” summarizing the basic statistics of the data sets, such as quartiles, medians and means, is computed at different time intervals  $\Delta t$ , and stored in the MySQL database system. As an example, Fig. 5 shows the database table “usa\_3” which summarizes the data sets collected by the USA-1 anemometer over time intervals of every 3 seconds ( $\Delta t = 3$  s) as indicated by the suffix “\_3”. Further statistics of the data sets are also summarized at 60 seconds, 6 minutes, 10 minutes, 30 minutes, and 6 hours. The recorded monitoring data – both secondary and tertiary monitoring data – serves as the data source used for analyzing the structural and operational states of the wind turbine.

The secondary and tertiary monitoring data is available to authorized human users and software programs via remote connections to the MySQL database system. In addition, a web interface is available, which provides a graphical user interface (GUI) and functions for remotely visualizing, analyzing, and downloading the monitoring data. The web interface, also installed at ICE in Bochum, is implemented as a web service written in Java. The web service is based on Adobe Flex, an open-source framework for developing Rich Internet Applications (RIAs) using the Adobe Flash platform (Adobe 2007, Polanco and Pedersen 2009). Fig. 6 depicts the GUI of the web interface that enables remote access to the integrated monitoring system. As shown in the left pane of the figure, the monitoring data is graphically displayed, as selected by the user through the checkboxes on the menu list in the control panel on the right hand side. Here, a time history of acceleration data over 24 hours is exemplarily displayed, collected by a Spider8 measuring unit through a 3D accelerometer (sensor B<sub>1</sub>). Using the control panel, the user can select the monitoring data collected by specific sensors, specify the time intervals to be plotted, conduct online data analyses, and export the data sets. From the selected sensor data in the illustrative example, it can be seen that the acceleration response varies significantly in the 24-hour time frame, which is due to the diurnal variations in the wind field acting on the wind turbine (Park *et al.* 2013).

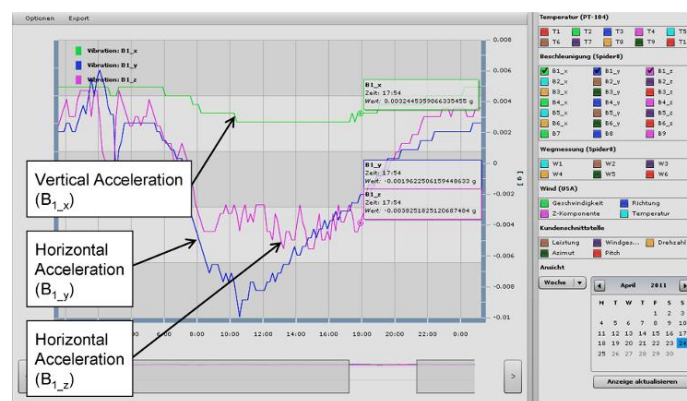


Fig. 6 Remote visualization of monitoring data through the GUI provided by the web interface



#### 4. Multiagent-based self-diagnostic system

A multi-agent system is designed for detecting malfunctions of the integrated monitoring system. If not detected timely, malfunctions of sensors and DAUs may cause interruptions in data acquisition, entailing the loss of valuable monitoring data affecting reliability and availability of SHM systems. Typical reasons for such malfunctions of real-time SHM systems include communication problems due to long-distance lines, breakdowns of sensors or temporary power blackouts that affect the computer systems. The multi-agent system, once a malfunction is observed, reacts in time to enable corrective actions and informs the responsible individuals through email alerts about the malfunctions. The affected DAUs or sensor components can be restarted remotely or replaced immediately.

Multi-agent systems have proven their efficiency and reliability in a number of decentralized engineering applications (Mittrup *et al.* 2003, Bilek *et al.* 2003, Smarsly *et al.* 2011). Multi-agent systems are composed of multiple interacting software components, referred to as “software agents”, which can be characterized by two basic capabilities: Software agents are capable of acting *autonomously* and *flexibly*, which makes multi-agent technology well suited for implementing decentralized, real-time SHM applications. The term “autonomous” describes an agent’s ability to control its actions, to operate without any direct intervention by humans or other software systems, and to decide independently which actions are appropriate in order to achieve prescribed goals (Wooldridge 2009, Russell and Norvig 1995). In addition, a software agent possesses a set of “flexible” features as listed below (Wooldridge and Jennings 1995, Jennings and Wooldridge 1998).

- Reactivity: Software agents perceive their (monitored) environment and respond timely to environmental changes.
- Proactiveness: Instead of solely acting in response to changes in their environment, software agents take initiative and show goal-directed behavior.
- Social ability: Software agents are capable of interacting and cooperating with other software agents, and with human users as well, to perform a specific task in order to achieve their goals. In addition to exchanging data, as in conventional object-oriented software engineering, software agents have the ability to communicate using formally defined languages and ontologies.

The most relevant agent-based feature for autonomous malfunction detection within the integrated structural health monitoring system is reactivity: When a malfunction happens in the monitored environment (i.e., in the monitoring system), the software agents, in cooperation with each other, have to detect the malfunction, to analyze it, and to react in real time by executing appropriate actions such as generating email alerts to notify the responsible individuals.

The multi-agent system, installed at ICE in Bochum, is developed using the Java Agent Development Framework JADE and is implemented in accordance with the standards of the IEEE Foundation for Intelligent Physical Agents (FIPA) (Bellifemine *et al.* 2003, 2004, 2007). The multi-agent system hosts several software agents, two of which are responsible for administration purposes. First, the “agent management system (AMS) agent” exerts supervisory control over the multi-agent system and maintains a directory of all software agents. Second, the “directory facilitator (DF) agent” implements a yellow page service, allowing the software agents to advertise their services and to look up services offered by other agents. In addition to the agents responsible for administration tasks, a “data interrogator agent” is implemented for malfunction detection, and a “mail agent” for sending email alerts to the responsible individuals.



To detect malfunctions, the data interrogator agent analyzes the secondary monitoring data collected by the DAUs, which is stored in the monitoring database. Typically, DAU malfunctions that cause interruptions of the data acquisition process are implicitly indicated by anomalies in the data sets. One pattern that captures a plenitude of different malfunctions can be described by an unusually large number of consecutive identical sensor measurements, i.e., erroneously constant values, stored repeatedly instead of the actual measurements. To detect such an anomaly, the data interrogator agent extracts and analyzes the measurements stored in the monitoring database. For that purpose, a set of configuration files specifying interrogation parameters, database URL, database driver, sensor specification, interrogation intervals, etc., is predefined and stored in the multi-agent system (Smarsly *et al.* 2012). The agent-based connection to the monitoring database is realized through Java Database Connectivity (JDBC), an industry standard for database-independent connectivity between Java applications, such as software agents, and various database systems. Even though the monitoring database as well as the multi-agent system is installed within the same (secured) computer network at the ICE in Bochum, the security of database requests and data transmissions is further ensured by security mechanisms provided by the MySQL database system, which requires password and username as well as secure drivers to be specified by the data interrogator agent.

Once the data interrogator agent has detected an anomaly, the individuals are immediately notified by the mail agent. The interaction between the data interrogator agent and the mail agent carried out for email notification is shown in Fig. 7. Upon receiving a message from the data interrogator agent, the mail agent collects all data necessary for composing the emails from the monitoring system. Metadata required for sending the emails (such as email server to be used or email addresses of the individuals responsible for the malfunctioning devices) is stored in configuration files also located in the multi-agent system. The email content, i.e. details on the malfunction detected, is implicitly provided by the data interrogator agent. To ensure secure email messages, the mail agent, similar to a human user, is user- and password-authenticated when trying to access the email server. Upon sending the emails, the mail agent, finalizing the agent interaction, informs the data interrogator that the emails have been sent.

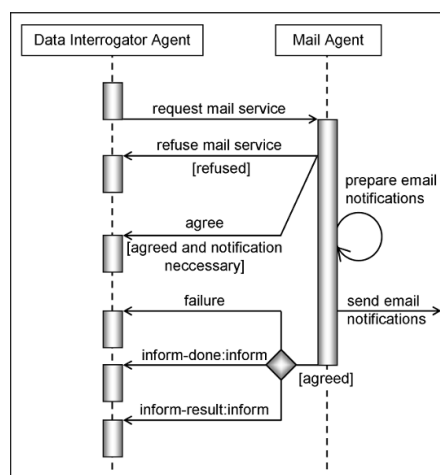


Fig. 7 FIPA-compliant agent interaction executed for email notification

Since its initial deployment in 2009, the multi-agent system has reliably detected the malfunctions occurred and has notified the human individuals via email alerts. To illustrate its operation, the detection of a malfunction of a temperature DAU as occurred on August 12, 2012, is shown in Fig. 8. As can be seen from Fig. 8, identical temperature measurements have been repeatedly stored by the DAU for a long period of time. As a direct consequence of the anomaly, the responsible engineers have instantaneously been informed by the multi-agent system via email. Fig. 9 shows an excerpt of the corresponding email, assembled and sent by the mail agent, which includes detailed information about the anomaly. An internal system malfunction in a DAU (one of the PT-104 input modules installed in the wind turbine) was identified as the cause and the engineers, after having received the email alert, remotely restarted the DAU in a timely manner.

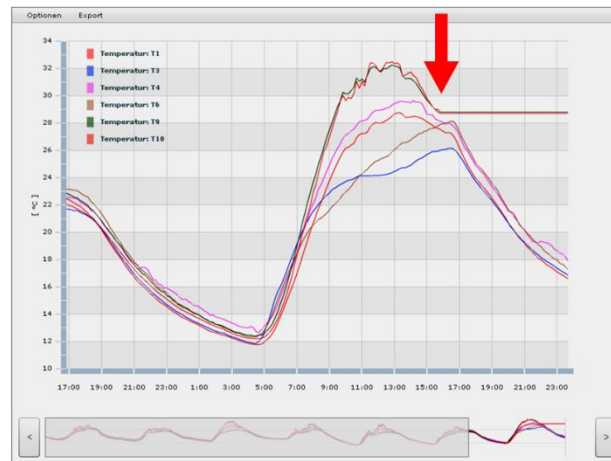


Fig. 8 Malfunction detected by the multi-agent system on August 12, 2012

```

From: monitoring@inf.bi.ruhr-uni-bochum.de
Date: 12 Aug 2012 19:52:57 +0200 (CEST)
Subject: [Generated Email] Wind Turbine Safety Report
To: smarsly@stanford.edu, [redacted]

-----
This email has autonomously been generated
and was sent by a software agent. Do not reply.
-----

(...)
Number of values observed per sensor: 86400
Number of significant values: 150
Sensors analyzed: t1;t2;t3;t4;t5;t6;t7;t8;t9;t10;

Anomaly detected:
Database: lwea
DAU id: pt104
Date: Sun Aug 12 17:46:21 CEST 2012
Sensor: t9
Errornumber: 28.757

Anomaly detected:
Database: lwea
DAU id: pt104
Date: Sun Aug 12 17:46:21 CEST 2012
Sensor: t10
Errornumber: 28.673

```

Fig. 9 Extract of the email alert, assembled and sent by the multi-agent system

## 5. Model updating

One key feature of the integrated monitoring system is the coupling of numerical wind turbine models and actual monitoring data taken from the physical structure. Finite element models of the wind turbine (including blades, nacelle, tower, and foundation) are created and validated using the recorded monitoring data. The model parameters are varied until the wind turbine model approximates the behavior of the physical wind turbine structure. For that purpose, the optimization framework “Multi-method Optimization PACKage (MOPACK)”, developed at ICE, is used (Nguyen *et al.* 2010).

### 5.1 Finite element modeling of the structural wind turbine system

In this study, the ANSYS finite element software is deployed to model the structural and dynamic behavior of the wind turbine (ANSYS 2011). Two finite element models of the wind turbine are developed. As shown in Fig. 10, the first finite element model includes the wind turbine tower and the rotor blades. Also, details of the structure, such as connection flanges between individual tower segments and the tower entrance door, are captured. The tower elements are modeled with three-dimensional 8-node finite shell elements (ANSYS-SOLSH190 elements), while the rotor blades are composed of multi-level shell elements (ANSYS-SHELL99 elements) to represent the sandwich character of the blades. Since blade design is often considered proprietary information by the wind turbine manufacturers, this study assumes that the entire cross-section of the rotor blades is made of fiber-glass reinforced material (Baumgart 2001). The outer skin panel of the rotor blades has a sandwich construction, and the inner parts of the blades are characterized by longitudinal struts stiffening the blades against shear stresses. All together, the complex 3D finite element model, which is intended to provide a highly accurate and realistic model of the wind turbine structure, consists of about 4,000 elements.

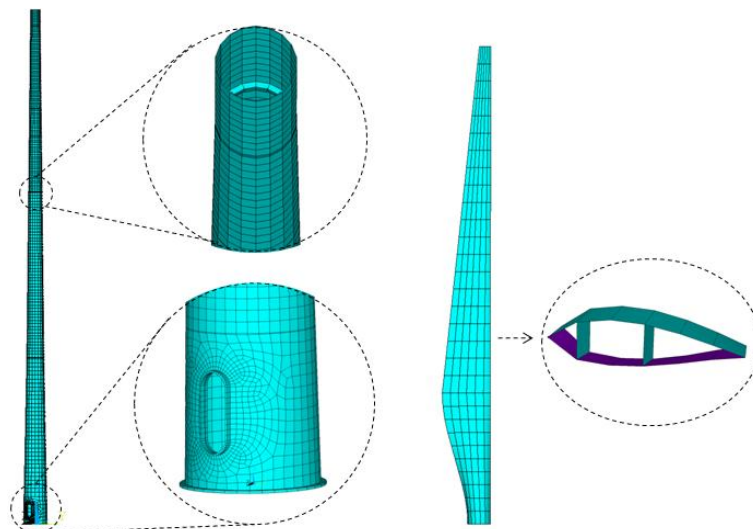


Fig. 10 Complex finite element model of the wind turbine

The second (simplified) finite element model (Fig. 11) includes only the wind turbine tower and rotor blades and is primarily composed of 3D beam elements (ANSYS-BEAM44 elements). In addition, the weight of the nacelle is captured by an extra mass placed on top of the tower. Assuming continuous elastic support for the ground, the behavior of the wind turbine foundation and the soil is modeled as an elastic foundation. In total, the simplified finite element model is composed of only 23 beam elements for the tower and 20 beam elements for the rotor. The reduced model is necessary and mandatory for the subsequent system identification because of computational demands. A verification process is conducted with the two finite element models to ensure that the modal characteristics of the simplified beam model match with those of the complex shell model. The determination of the relevant modal parameters using the first model takes about 3 hours, while the calculations using the second model take about 10 minutes.

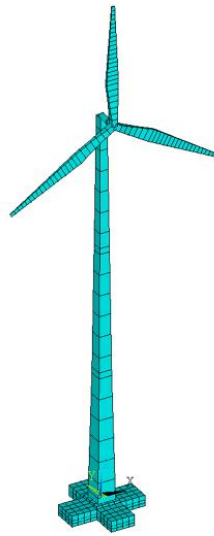


Fig. 11 Simplified finite element model

## 5.2 Determination of modal parameters and system identification

The determination of modal parameters is accomplished by modifying the properties of the finite element models, such as stiffnesses, masses, geometries, elements of the inertia tensor, and damping values. These modifications are repeated until the computed structural responses of the models, e.g., accelerations, velocities and displacements, approximate closely the measured responses of the monitored wind turbine. If the approximation problem is posed as an optimization problem minimizing the differences between the computed and measured responses, the problem becomes an inverse or system identification problem with a moderate number of optimization variables.

In the integrated monitoring system, the numerical solution of the inverse problem is carried out by minimizing the difference between (a) the structural response data calculated from the second finite element model through finite element analysis (FEA) and (b) the corresponding structural response data determined from the actual measurements taken from the wind turbine.

For determining the modal parameters of interest from the finite element model (natural frequencies and bending modes), free vibration analyses are conducted in ANSYS. By contrast, the calculation of the modal parameters from the actual measurements is based on Operational Modal Analysis (OMA). The objective of OMA, also known as Output-Only Modal Analysis, is to determine modal parameters based on the system responses without knowledge about the excitation input. For the wind turbine, the excitation input, i.e. the wind loading, can not be measured accurately and is therefore assumed to be Gaussian white noise.

The OMA-based modal analyses are performed using the commercial software “ARTEMIS Extractor” (SVS, 2011). Specifically, two OMA methods are used: (i) The Enhanced Frequency Domain Decomposition Method (EFDD) in the frequency domain and (ii) the Stochastic Subspace Identification Method (SSI) in the time domain. As illustrated in the previous sections, the system responses of the wind turbine needed for the OMA analyses, such as accelerations and displacements, are measured in real-time by the on-site hardware system and stored in the monitoring database being part of the decentralized software system. The system responses, as shown in Fig. 6, are remotely downloaded from the monitoring database in different time windows. Drifts in the accelerations due to temperature fluctuations are eliminated and the system responses are analyzed using ARTEMIS Extractor. Illustrating the first three bending modes of the wind turbine in the X-Z- and Y-Z-plane, Fig. 12 shows the analysis results of the measurement-driven EFDD and SSI method together with the FEA-based results predicted by the finite element model.

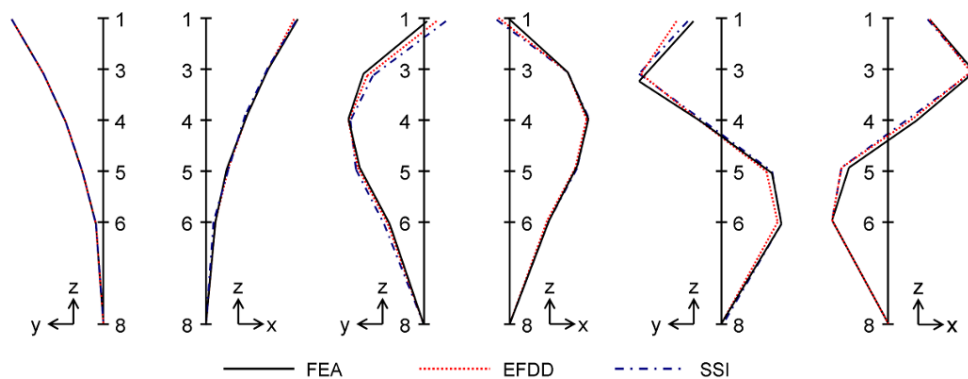


Fig. 12 First three bending modes of the turbine in X-Z- and Y-Z-plane computed by FEA (black, full) and identified by EFDD (red, dotted) and SSI (blue, dash-dotted)

To investigate the validity of the implemented finite element models, Table 1 compares the model-predicted eigenfrequencies calculated from FEA with the measurement-driven EFDD and SSI calculations. In addition, Figs. 13 and 14 show the consistency between model-predicted and measurement-driven results using the Modal Assurance Criterion (MAC). MAC is a statistical indicator (Allemang 2003) that assumes values between 0 (indicating no consistency) and 1 (indicating consistency). With values between 0.9636 and 0.9998, the diagonals of the MAC matrices tend towards 1, which indicates high correlation between the FEA-based eigenfrequencies and those based on the measurement data.

Table 1 Comparison of 6 parameters: Computed by FEA vs. identified by EFDD and SSI methods

	Mode Computed	Measured (EFDD)				Measured (SSI)			
	FEA	EFDD	Diff <sub>EFDD</sub>		MAC	SSI	Diff <sub>SSI</sub>		MAC
	$f$ (Hz)	$f$ (Hz)	(%)	$d$ (%)	FEA-EFDD	$f$ (Hz)	(%)	$d$ (%)	FEA-SSI
1 (X-Z)	0.3599	0.3859	7.2	7.587	0.9984	0.3510	2.5	4.073	0.9981
2 (Y-Z)	0.3612	0.3860	6.9	7.561	0.9998	0.3753	4.0	1.118	0.9997
3 (Y-Z)	2.250	2.222	1.2	1.773	0.9905	2.456	9.2	1.744	0.9636
4 (X-Z)	2.437	2.226	8.7	1.907	0.9927	2.244	7.9	1.882	0.9889
5 (Y-Z)	5.713	5.593	2.1	4.292	0.9809	5.455	4.5	1.492	0.9905
6 (X-Z)	6.258	5.832	6.8	3.627	0.9907	5.597	10.6	1.476	0.9711

$f$ =frequency,  $d$ =damping,  $\text{Diff}_{\text{EFDD}} = |f_{\text{FEA}} - f_{\text{EFDD}}| / f_{\text{FEA}}$ ,  $\text{Diff}_{\text{SSI}} = |f_{\text{FEA}} - f_{\text{SSI}}| / f_{\text{FEA}}$

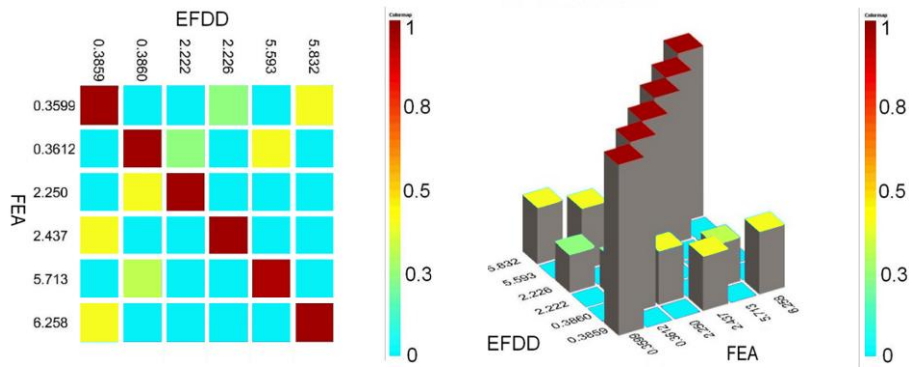


Fig. 13 MAC matrix: Comparison of eigenfrequencies from EFDD with FEA

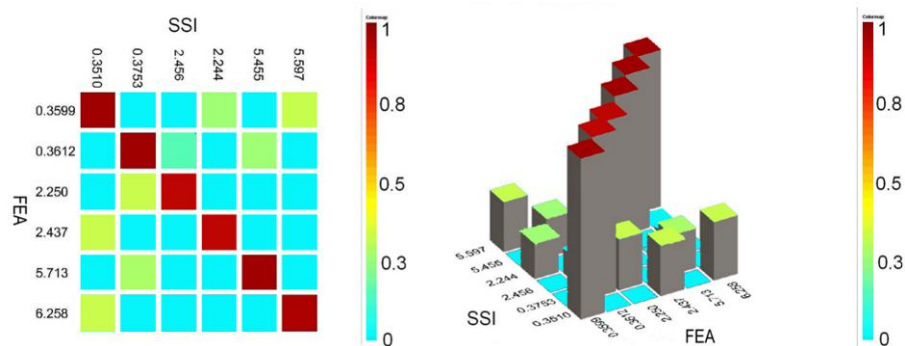


Fig. 14 MAC matrix: Comparison of eigenfrequencies from SSI with FEA

### 5.3 Model updating and damage detection

As demonstrated in the preceding subsection, the model-predicted and the measurement-driven modal parameters match almost exactly, i.e., the modal parameters calculated from the implemented finite element models correspond well with the measured responses, i.e., the assumed “unknown” physical parameters used in the finite element models correspond sufficiently with the properties of the real wind turbine. In this case, no further model updating is required. Otherwise, the parameters of the finite element models are repeatedly varied within an iterative optimization procedure until the differences are minimal or as small as prescribed.

With respect to the identification of deteriorations or damages, it should be noted that it can neither be anticipated nor be expected that any serious damage events have occurred to the 12-year old wind turbine within the limited time window of a 36-month research project. Therefore, in current research, synthetic damage patterns are imposed on the finite element wind turbine model to predict the structural response, which means that specified damage is systematically created, analyzed, and archived in a “damage catalog”. If deteriorations or damages occur to the real wind turbine in the future, the a priori created damage patterns allow a rapid and reliable damage assessment. The construction of the damage catalogue is briefly illustrated in the following paragraphs by the example of a specific damage scenario. In this damage scenario, the loosening of high-strength bolts of the connection flanges of the wind turbine tower is exemplarily shown. The damage scenario is mapped by introducing four stiffness reducing parameters that are the optimization variables of interest. Four parameters on the bending stiffnesses, apparently appropriate damage indicators, are introduced as shown in Fig. 15, because the tower consists of three individual segments that are joined to each other as well as to the foundation and to the nacelle. In other words, to simulate the deterioration behavior imposed by the loss of bolt pre-stressing, four suitable spring elements are introduced into the finite element model, at the height of the four flanges connecting the segments.

As noted by Zhang *et al.* (2007), besides a proper definition of the optimization variables, both the definition of a tailor-made objective function and a robust optimization procedure are prerequisite to model updating. In this paper, the objective function suggested by Bittner (2008) is adopted: Defining  $x_i$  as the  $i$ th updating parameter, the model updating problem is a constrained non-linear optimization problem where  $\mathbf{x} = \{x_1, x_2, x_3, x_4\}$  are the optimization variables according to the damage scenario illustrated in Fig. 15. Focusing on the modal properties of the wind turbine – i.e., the natural frequencies  $\omega_i$  and natural mode shapes  $\phi_i$  – in a representative frequency range of the monitoring data, two error expressions are defined. The first error expression  $\varepsilon_{1,i}(\mathbf{x})$  is defined as a function of the measured eigenfrequencies  $\omega_{m,i}$  and the computed eigenfrequencies  $\omega_{n,i}$  as denoted in Eq. (1). The second error expression  $\varepsilon_{2,i}(\mathbf{x})$  is established using the aforementioned MAC values in terms of weighting factors, which represents the scalar error of the measured mode shapes  $\phi_{m,i}$  and the computed mode shapes  $\phi_{n,i}$  (Eq. (2))

$$\varepsilon_{1,i}(\mathbf{x}) = \left\| \frac{\omega_{m,i} - \omega_{n,i}(\mathbf{x})}{\omega_{m,i}} \right\| \quad (1)$$

$$\varepsilon_{2,i}(\mathbf{x}) = \text{MAC}(\phi_{m,i}, \phi_{n,i}(\mathbf{x}))^2 \quad (2)$$

Then, the objective function  $f(\mathbf{x})$  to be minimized is given by



$$f(\mathbf{x}) = \frac{\sum_i \varepsilon_{1,i}(\mathbf{x}) \varepsilon_{2,i}(\mathbf{x})}{\sum_i \varepsilon_{2,i}(\mathbf{x})} \quad (3)$$

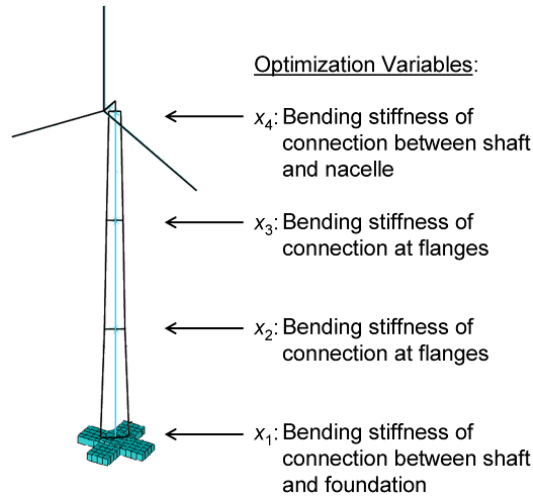


Fig. 15 Optimization variables in the damage scenario

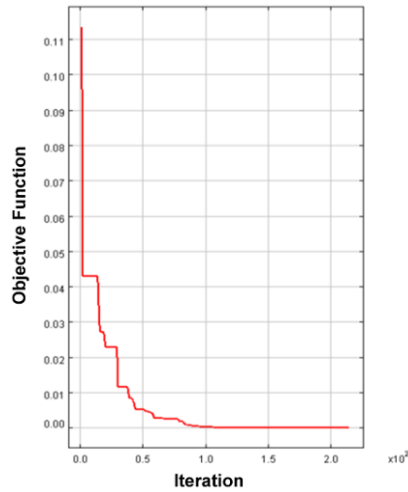


Fig. 16 Optimization history using ES applying the optimization criterion according to Bittner (2008)

It can be seen that the objective function  $f(\mathbf{x})$  is non-linear as well as discontinuous representing a non-standard optimization problem to be solved. Evolution Strategies (ES) and Differential Evolution (DE) have been proven to be one of the most efficient optimization methods to solve non-linear, multi-modal and non-standard optimization problems (Bäck 1996, Stangenberg *et al.*

2009). Both strategies are implemented in the aforementioned optimization framework MOPACK being part of the integrated monitoring system. MOPACK, a Java-based optimization framework that integrates numerous optimization strategies such as Evolution Strategies and Differential Evolution (Nguyen *et al.* 2010), is interfaced with the finite element software used (ANSYS in this study). According to the optimization strategy chosen, the finite element analyses using ANSYS are carried out repeatedly in a MOPACK-driven optimization loop to compute the required quantities, i.e., the dynamic response, employed in the objective function. For the example damage scenario – the loosening of a specific high-strength bolt – the optimization history using Evolution Strategies is illustrated in Fig. 16.

## 6. Management module

Installed on a computer at the Engineering Informatics Group (EIG) at Stanford University, the management module supports the wind turbine life-cycle management through remote analyses of monitoring data, i.e., structural, environmental, and operational wind turbine data; it provides algorithms, for example, for calculating tip speed ratios of wind turbines, constructing wind turbine power curves, computing power coefficients, and analyzing wind speed distributions. In addition, the management module allows studying correlations in the monitoring data and detecting significant changes in the operational and structural wind turbine condition. For that purpose, a variety of statistical methods is implemented to accommodate the specific needs of wind turbine life-cycle management. The architecture and the core classes of the management module, written in Java, are shown in Fig. 17 by means of an abbreviated UML class diagram. The basic architecture includes three separate tiers, allowing any tier to be upgraded, changed or replaced independently from each other. The first tier, the *presentation*, provides user access to the management module and can be installed on any PC, laptop, or Java-enabled mobile devices such as cell phones and smart phones. The *data access* tier is designed to remotely access the data from the monitoring database installed at ICE in Bochum. The third tier, the *controller*, contains specific algorithms (e.g. fast Fourier transforms, statistical variance analyses, etc.) to be used for structural as well as operational life-cycle analyses of the wind turbine.

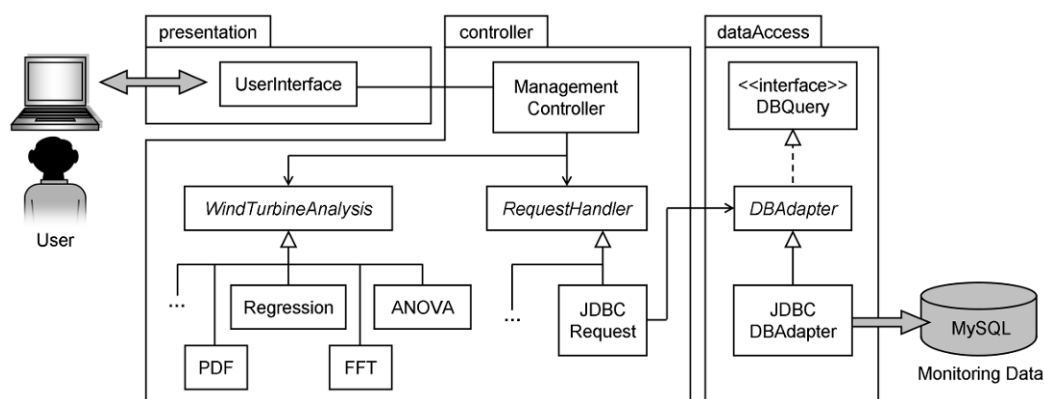


Fig. 17 Architecture of the management module

In the following paragraphs, life-cycle analyses are presented to exemplarily illustrate the rapid online assessment of the operational efficiency and structural performance of the wind turbine. The online data analyses performed can help not only to understand the operational behavior and the structural condition of the wind turbine, but also to validate particular measures undertaken to optimize the operational performance, to quantify energy losses that usually remain undetected, and to minimize the costs for operation and maintenance. To demonstrate the functionality and the practicability of the management module, two case studies are shown; the first case study focuses on the wind turbine's operational efficiency, and the second case study considers the structural performance of the wind turbine.

To assess the wind turbine operational efficiency, power curves are exemplarily constructed based on one-month monitoring data recorded in March 2010, March 2011 and March 2012 (Fig. 18). The curve provided by the wind turbine manufacturer is also shown in the figure. The power curves are calculated by the management module based on the power output and the wind speed measurements available in the integrated monitoring system. As can be seen from Fig. 18, the results show that no significant changes can be observed when comparing the measurement-based power curves of 2010, 2011 and 2012. Furthermore, the power curve provided by the manufacturer matches the actual measurement-based power curves for the normal operational wind speeds.

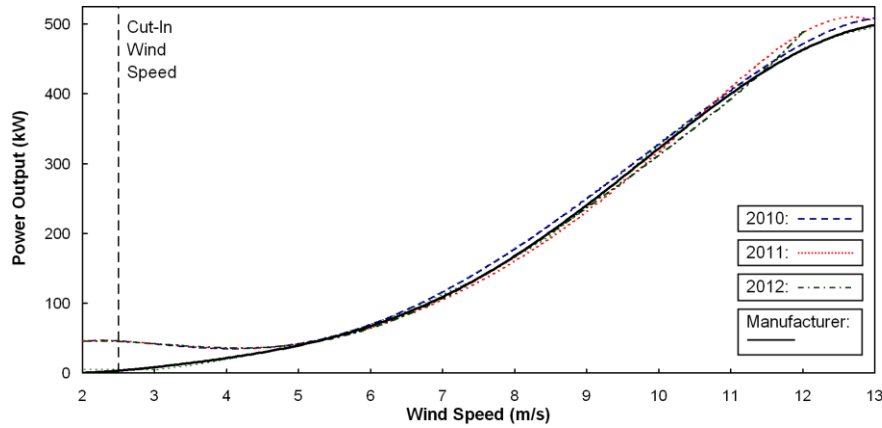


Fig. 18 Power curves of the wind turbine in March 2010, 2011, and 2012 calculated from monitoring data

Fig. 19 illustrates the actual wind turbine efficiency by means of power coefficients  $C_P$ , which are plotted as a function of the wind speed. The power coefficients, defined as the power extracted by the wind turbine relative to the power available in the wind stream, are calculated by the management module as

$$C_P = \frac{P}{0.5\rho AV^3} \quad (4)$$

where  $P$  is the power output,  $\rho$  is the air density assuming  $\rho = 1.225 \text{ kg/m}^3$ ,  $V$  is the wind speed measured by the monitoring system, and  $A$  is the swept area of the wind turbine calculated from the rotor diameter. In addition to the  $C_P$  curves, the Betz limit, representing the theoretical

maximum of power efficiency, is shown in Fig. 19, which implies that no wind turbine can convert more than 59.3% of the kinetic energy of the wind into mechanical energy. The efficiency of the wind turbine, as a result of this example calculation, is largest at the optimum wind speed  $V = V(C_{P,max})$  that is found between  $V = 7.5$  m/s and  $V = 8.5$  m/s in each of the regarded one-month time spans.

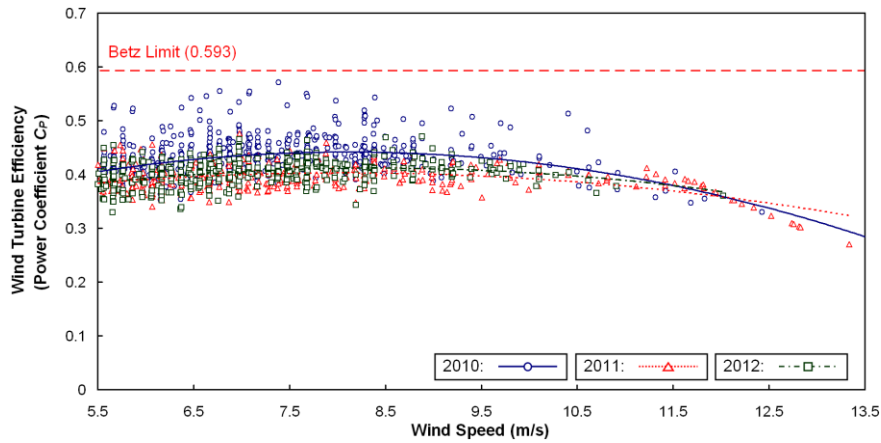


Fig. 19 Wind turbine efficiency in March 2010, 2011 and 2012

In addition to the operational efficiency of the wind turbine, the structural condition is assessed: In a three-step process, a comparison of the structural responses at two different dates in the wind turbine's service life is conducted. First, typical site-specific loading conditions (i.e., typical environmental conditions) are computed based on the monitoring data to achieve comparable load cases that represent normal operation. Second, two distinct points in time at which the loading conditions act on the wind turbine are determined through a search in the monitoring database. Finally, the structural responses of the wind turbine are compared. Typical loading conditions are defined by average air temperature and a characteristic mean wind profile for the given site. In addition, the wind direction and – because of the atmospheric stability – the time of the day is considered. Whereas average air temperature and wind direction are calculated directly from the monitoring data, the mean wind profile is estimated by the management module applying the wind profile power law (Rai *et al.* 2011, Sathe and Bierbooms 2007) given by Eq. (5)

$$\frac{V_N}{V_{USAI}} = \left( \frac{h_N}{h_{USAI}} \right)^\alpha \quad (5)$$

where  $V_N$  is the wind speed at  $h_N = 67$  m measured and corrected by the nacelle anemometer,  $V_{USAI}$  is the wind speed at  $h_{USAI} = 13$  m measured by the ultrasonic anemometer being part of the on-site hardware system, and  $\alpha$  is the power exponent calculated by the management module using the wind speed values and the given heights. The characteristic loading conditions are summarized in Fig. 20. By searching in the monitoring database, two points in time are identified – in May 2012 and in October 2012 as listed in Table 2 – at which the characteristic loading conditions apply.

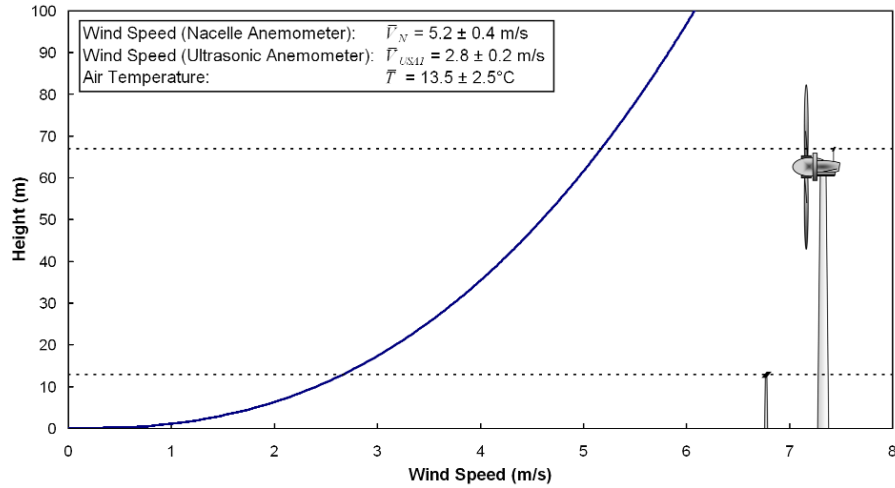


Fig. 20 Site-specific loading conditions used for comparison of the structural response

Table 2 Results of the database search

	$V_N$ (m/s)	$V_{USAI}$ (m/s)	$T$ (°C)	$\theta$ (°)	Time of day
May 18, 2012	5.6	2.9	13.0	163.0	07:51:40
Oct 11, 2012	5.6	2.8	10.9	134.0	10:45:20

$V_N$ =wind speed (nacelle anemometer),  $V_{USAI}$ =wind speed (ultrasonic anemometer),  $T$ =air temperature,  $\theta$ =wind direction

The corresponding wind turbine responses recorded at both dates are depicted in Fig. 21 exemplarily by means of 20-second time history plots that distinctively reflect the typical structural response. The plots show time histories of the longitudinal strain of the wind turbine tower, as calculated from the displacement measurements recorded by sensors  $W_3$  (21 m level) and  $W_6$  (42 m level) as well as the lateral vibration of the tower recorded by accelerometer  $B_1$  (62 m level). In total, the structural responses at both dates are in close agreement; the strain time history data shows very good agreement in the time domain, as has been computed through a rainflow counting algorithm (Matsuishi and Endo 1968) over about 2,000 cumulative cycles. To quantify the frequency response, the acceleration time history data is transferred to the frequency domain using the Cooley-Tukey fast Fourier transform (FFT) algorithm (Cooley and Tukey 1965). The Fourier spectra calculated from the acceleration data, representing the frequency response function of the wind turbine, are shown in Fig. 22. A peak-picking (PP) algorithm, representing a relatively simple but computational efficient method for identifying modal properties, is used to determine high-valued spectrum peaks from the frequency spectra and for determining the natural frequencies of the wind turbine.

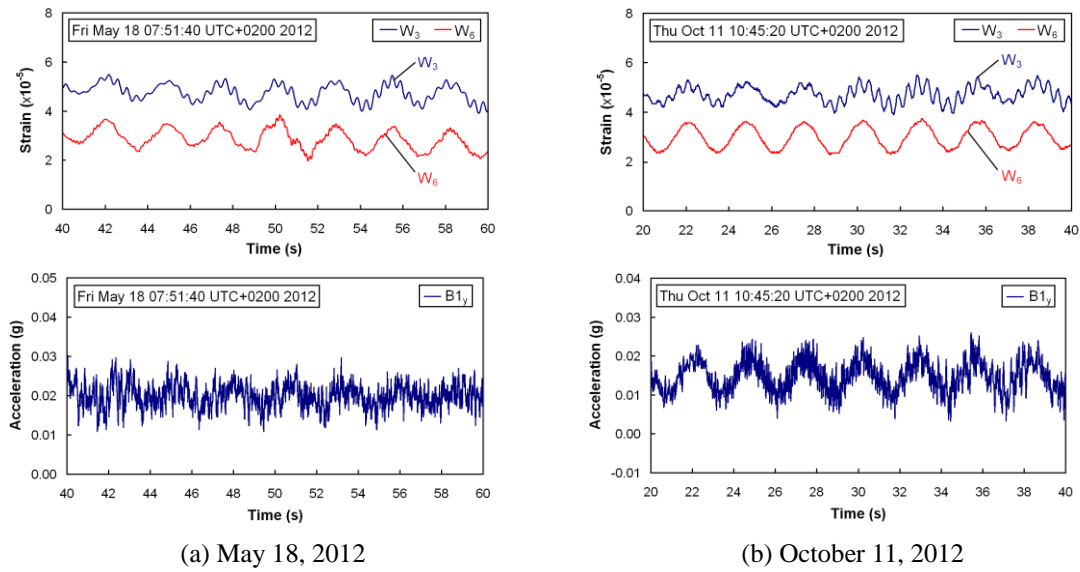


Fig. 21 Wind turbine response data

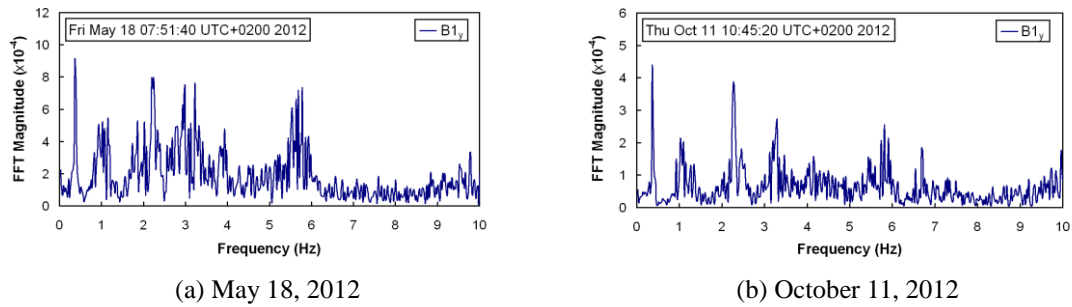
Fig. 22 FFT results obtained from sensor  $B_1$ 

Table 3 Comparison of modal parameters

Mode shape	Oct 11, 2012	May 18, 2012		FE model	
	$f$ (Hz)	$f$ (Hz)	(%)	$f$ (Hz)	(%)
1	0.366	0.366	0.0	0.361	1.3
2	2.271	2.271	0.0	2.250	0.9
3	5.786	5.811	0.4	5.713	1.3

Comparing the natural frequencies calculated from the data obtained in May 2012 and in October 2012, Table 3 shows that the first two natural frequencies match well and that only the third natural frequency shows a minor and insignificant discrepancy (0.4%). In addition to

comparing the natural frequencies at both selected dates, the finite element model introduced in section 5 is validated: As can be seen from Table 3, the results obtained from the finite element model, with deviations in the frequencies between 0.9% and 1.3%, show close agreement with those calculated from the monitoring data.

## **7. Conclusions**

Wind energy technology, providing inexpensive, clean, and safe energy, represents one of the fastest growing markets within the emerging sector of renewable energy systems. With respect to an economic life-cycle management of wind turbines, knowledge about the structural condition and the operational efficiency of wind turbines is essential to ensure that components of wind turbines can timely be replaced, maintenance and repair work can economically be scheduled, and expensive downtime can be reduced. In this paper, an integrated monitoring system for wind turbines has been presented. The integrated system, as described in the paper, consists of different subsystems designed for long-term structural health monitoring, self-detection of system malfunctions, continuous finite element model updating, and life-cycle management wind turbines.

The system is in service since 2009, continuously monitoring a 500 kW wind turbine in Germany. As has been demonstrated in this paper, using monitoring data for structural assessment and life-cycle management significantly facilitates the understanding of both the structural and operational behavior of wind turbines. According to the analyses exemplarily conducted on the wind turbine, there has no decrease in the operational efficiency been detected and no significant changes in the structural condition have been found in the regarded time period.

The main objective of this study is to demonstrate the feasibility of the integrated approach and the reliability of the implemented monitoring system. Many opportunities exist to further improve the proposed concepts and to extend the capabilities of the integrated monitoring and management framework. For example, the multiagent-based self-diagnostic system can be extended by additional software agents that are able to detect other types of sensor or DAU malfunctions and to support fault tolerance in SHM systems. Also, the research can further be extended to transfer the proposed concepts from monitoring of a single wind turbine to wind farm monitoring (and control). In this respect, the results of this research may serve as a basis to facilitate cost-efficient operation and life-cycle management of more complex, interconnected wind energy systems on the network level.

## **Acknowledgments**

This research is partially funded by the German Research Foundation (DFG) under grants SM 281/1-1 and SM 281/2-1, awarded to Dr. Kay Smarsly, and grant HA 1463/20-1, awarded to Professor Dietrich Hartmann. This research is also partially supported by the U.S. National Science Foundation (NSF) through grant CMMI-0824977, awarded to Professor Kincho H. Law. Any opinions, findings, conclusions, or recommendations expressed are those of the authors and do not necessarily reflect the views of the DFG and the NSF.



## References

- Adobe Systems Incorporated (2007), *Datasheet Adobe Flex Builder 3 – Create engaging, cross-platform rich Internet applications*, San Jose, CA, USA: Adobe Systems Incorporated.
- Allemang, R.J. (2003), “The Modal Assurance Criterion (MAC): twenty years of use and abuse”, *Sound Vib.*, **37**(8), 14-21.
- Amirat, Y., Benbouzid, M.E.H., Bensaker, B. and Wamkeue, R. (2007), “Condition monitoring and fault diagnosis in wind energy conversion systems: a review”, *Proceedings of the IEEE International Electric Machines and Drives Conference*. Antalya, Turkey, May 3-5.
- ANSYS Inc. (2011), *Documentation for ANSYS*, Documentation. Canonsburg, PA, USA: ANSYS Inc.
- Avendano-Valencia, L.D., Spiridonakos, M.D. and Fassois, S.D. (2011), “In-operation identification of a wind turbine structure via non-stationary parametric models”, *Proceedings of the 8th International Workshop on Structural Health Monitoring*. Stanford, CA, USA, September 13-15.
- Bäck, T. (1996), *Evolutionary algorithms in theory and practice*, New York, NY, USA: Oxford University Press.
- Baumgart, A. (2001), *Models for wind turbines – a collection*, Riso-R-1352(EN), Roskilde, Denmark: Riso National Laboratory.
- Bellifemine, F., Caire, G., Pogg, A. and Rimassa, G. (2003), “JADE – a white paper”, *EXP Online*, **3**(3), 6-19.
- Bellifemine, F., Caire, G. and Greenwood, D. (2004), *Developing Multi-Agent Systems with JADE*, Hoboken, NJ, USA, John Wiley & Sons.
- Bellifemine, F., Caire, G., Trucco T. and Rimassa, G. (2007), *Jade Programmer's Guide*. [Online] Available at <http://jade.tilab.com/doc/programmersguide.pdf>.
- Besnard, F. (2009), *On optimal maintenance management for wind power systems*, Licentiate Thesis. Stockholm, Sweden: KTH Royal Institute of Technology.
- Bilek, J., Mittrup, I., Smarsly, K. and Hartmann, D. (2003), “Agent-based concepts for the holistic modeling of concurrent processes in structural engineering”, *Proceedings of the 10th ISPE International Conference on Concurrent Engineering: Research and Applications*. Madeira, Portugal, June 26-30.
- Bittner, U. (2008), “Successive model-updating of the dynamic behavior of casing bodies on a practical example of an axial piston pump”, *Proceedings of the NAFEMS Seminar Interaction of Simulation and Testing: New Requirements and New Opportunities in Structural Dynamics*. Wiesbaden, Germany, November 12-13.
- Castors, M. (2008), *PDI Performance tuning check-list*, Technical Report. Orlando, FL, USA, Pentaho Corporation.
- Ciang, C.C., Lee, J.R. and Bang, H.J. (2008), “Structural health monitoring for a wind turbine system: a review of damage detection methods”, *Meas. Sci. Technol.*, **19**(12), 122001 (20 pages).
- Cooley, J.W. and Tukey, J.W. (1965), “An algorithm for the machine calculation of complex fourier series”, *Math. Comput.*, **19**(90), 297-301.
- Echavarria, E., Hahn, B., van Bussel, G.J.W. and Tomiyama, T. (2008), “Reliability of wind turbine technology through time”, *J. Sol. Energ.-T. ASME*, **130**(3), 031005 (8 pages).
- EIA (U.S. Energy Information Administration) (2011), *International Energy Outlook 2010 – Highlights*. Report. Washington, DC, USA, U.S. EIA.
- Feinberg, S. (2011), *Clean energy investment storms to new record in 2010*, Press release. January 11, 2011. [Online] Available at <http://bnef.com/PressReleases/view/134>.
- Hameed, Z., Hong, Y.S., Cho, Y.M., Ahn, S.H. and Song, C.K. (2009), “Condition monitoring and fault detection of wind turbines and related algorithms: a review”, *Renew. Sust. Energ. Rev.*, **13**(1), 1-39.
- Hartmann, D. and Höffer, R. (2010), *Lifespan assessment of wind turbines through system identification (Lebensdauerabschätzung von Windenergieanlagen mit fortlaufend durch Systemidentifikation aktualisierten numerischen Modellen)*, Research project funded by the German Research Foundation (DFG) through the research grant HA 1463/20-1. Ruhr University Bochum, Bochum, Germany.
- Hartmann, D., Smarsly, K. and Law, K.H. (2011), “Coupling sensor-based structural health monitoring with

- finite element model updating for probabilistic lifetime estimation of wind energy converter structures”, *Proceedings of the 8th International Workshop on Structural Health Monitoring*. Stanford, CA, USA, September 13-15.
- Hyers, R.W., McGowan, J.G., Sullivan, K.L., Manwell, J.F. and Syrett, B.C. (2006), “Condition monitoring and prognosis of utility scale wind turbines”, *Energy Mater.*, **1**(3), 187-203.
- Jennings, N.R. and Wooldridge, M. (1998), “Applications of intelligent agents”, (Eds., N.R. Jennings and M. Wooldridge), *Agent technology: foundations, applications, and markets*. Berlin, Germany, Springer.
- Lachmann, S., Baitsch, M., Hartmann, D. and Höffer, R. (2009), “Structural lifetime prediction for wind energy converters based on health monitoring and system identification”, *Proceedings of the 5th European & African Conference on Wind Engineering*. Florence, Italy, July 19.
- Lu, B., Li, Y., Wu, X. and Yang, Z. (2009), “A review of recent advances in wind turbine condition monitoring and fault diagnosis”, *Proceedings of the IEEE Power Electronics and Machines in Wind Application*. Lincoln, NE, USA, June 24-26.
- Matsuishi, M. and Endo, T. (1968), “Fatigue of metals subjected to varying stress”, *Proceedings of the Kyushu District Meeting of the Japan Society of Mechanical Engineers*. Fukuoka, Japan, March.
- Mittrup, I., Smarsly, K., Hartmann, D. and Bettzieche, V. (2003), “An agent-based approach to dam monitoring”, *Proceedings of the 20th CIB W78 Conference on Information Technology in Construction*. Auckland, New Zealand, April 23-25.
- Nguyen, V.V., Hartmann, D., Baitsch, M. and König, M. (2010), “A distributed agent-based approach for robust optimization”, *Proceedings of the 2nd International Conference on Engineering Optimization*. Lisbon, Portugal, September 6-9.
- Nilsson, J. and Bertling, L. (2007), “Maintenance management of wind power systems using condition monitoring systems – life cycle cost analysis for two case studies”, *IEEE T. Energy Convers.*, **22**(1), 223-229.
- Rai, R.K., Singh, M.J. and Naughton, J.W. (2011), “Investigation of wind turbine response to various wind inflow models”, *Proceedings of the 49th AIAA Aerospace Sciences Meeting*. Orlando, FL, USA, January 4-7.
- Park, J., Smarsly, K., Law, K.H. and Hartmann, D. (2013), “Multivariate analysis and prediction of wind turbine response to varying wind field characteristics based on machine learning”, *Proceedings of the ASCE International Workshop on Computing in Civil Engineering*. Los Angeles, CA, USA, June 23-25.
- Polanco, J. and Pedersen, A. (2009), *Understanding the flex 3 component and framework lifecycle*, San Francisco, CA, USA, DevelopmentArc LLC.
- Ribrant, J. and Bertling, L.R. (2007), “Survey of failures in wind power systems with focus on Swedish wind power plants during 1997-2005”, *Proceedings of the IEEE Power Engineering Society General Meeting 2007*. Tampa, FL, USA, June 24-28.
- Roldan, M.C. (2009), *Pentaho data integration (Kettle) tutorial*, Technical Report. Orlando, FL, USA, Pentaho Corporation.
- Rolfes, R., Gerasch, G., Haake, G., Reetz, J. and Zerbst, S. (2006), “Early damage detection system for tower and rotor blades of offshore wind turbines”, *Proceedings of the 3rd European Workshop on Structural Health Monitoring*. Granada, Spain, July 5-7.
- Rolfes R., Zerbst S., Haake G., Reetz J. and Lynch J.P. (2007), “Integral SHM-System for Offshore Wind Turbines Using Smart Wireless Sensors”, *Proceedings of the 6th International Workshop on Structural Health Monitoring*. Stanford, CA, USA, September 11-13.
- Russell, S. and Norvig, P. (1995), *Artificial intelligence: a modern approach*, Englewood Cliffs, NJ, USA, Prentice-Hall.
- Sathe, A and Bierbooms, W (2007), “Influence of different wind profiles due to varying atmospheric stability on the fatigue life of wind turbines”, *J. Phys. Conf. Ser.*, **75**(1), 012056.
- Schneider, M., Froggatt, A. and Thomas, S. (2011), *The world nuclear industry status report 2010–2011, Nuclear Power in a Post-Fukushima World – 25 Years After the Chernobyl Accident*. Washington, DC, USA, Worldwatch Institute. [Online] Available at: [http://www.worldwatch.org/system/files/pdf/WorldNuclearIndustryStatusReport2011\\_%20FINAL.pdf](http://www.worldwatch.org/system/files/pdf/WorldNuclearIndustryStatusReport2011_%20FINAL.pdf).

- Smarasly, K. and Hartmann, D. (2009a), "Real-time monitoring of wind turbines based on software agents", *Proceedings of the 18th International Conference on the Applications of Computer Science and Mathematics in Architecture and Civil Engineering*. Weimar, Germany, July 7-9.
- Smarasly, K. and Hartmann, D. (2009b), "Multi-scale monitoring of wind energy plants based on agent technology", *Proceedings of the 7th International Workshop on Structural Health Monitoring*. Stanford, CA, USA, September 9-11.
- Smarasly, K. and Hartmann, D. (2010), "Agent-oriented development of hybrid wind turbine monitoring systems", *Proceedings of the 2010 EG-ICE Workshop on Intelligent Computing in Engineering*. Nottingham, UK, June 30 - July 2.
- Smarasly, K., Law, K.H. and Hartmann, D. (2012), "Multi-agent-based collaborative framework for a self-managing structural health monitoring system", *J. Comput. Civil Eng.*, **26**(1), 76-89.
- Smarasly, K., Law, K.H. and König, M. (2011), "Resource-efficient wireless monitoring based on mobile agent migration", *Proceedings of the SPIE (Vol. 7984): Health Monitoring of Structural and Biological Systems 2011*. San Diego, CA, USA, March 6-10.
- Stangenberg, F., Breitenbücher, R., Bruhns, O.T., Hartmann, D., Höffer, R., Kuhl, D. and Meschke, G. (Eds.) (2009), *Lifetime-oriented structural design concepts*, Berlin, Germany, Springer.
- SVS (Structural Vibration Solutions) (2011), *ARTEMIS software – version 5.3*, Aalborg East, Denmark: Structural Vibration Solutions A/S.
- Swartz, R.A., Lynch, J.P., Sweetman, B., Rolfes, R. and Zerbst, S. (2010), "Structural monitoring of wind turbines using wireless sensor networks", *Smart Struct. Syst.*, **6**(3), 183-196.
- Wooldridge, M. and Jennings, N.R. (1995), "Intelligent agents: theory and practice", *Knowl. Eng. Rev.*, **10**(2), 115-152.
- Wooldridge, M. (2009), *An introduction to multiagent systems*, 2nd Ed., Hoboken, NJ, USA, John Wiley & Sons.
- WWEA (World Wind Energy Association) (2012), *Report 2011*, Report. Bonn, Germany, WWEA.
- Zhang, X. Y., Sim, S. H. and Spencer Jr., B.F. (2007), "Finite element model updating of a truss model using incomplete modal data", *Proceedings of the World Forum on Smart Materials and Smart Structures Technology*. Chongqing, China, May 22-27.